

A Hierarchical Real-time Balancing Market Considering Multi-microgrids with Distributed Sustainable Resources

Yan Du, *Student Member, IEEE* and Fangxing Li, *Fellow, IEEE*

Abstract— A hierarchical market structure is proposed in this paper for multiple microgrids to participate in transmission-level real-time balancing markets and to provide ancillary services to the utility grid. At the distribution level, local microgrids with distributed sustainable resources, such as demand response, distributed renewables, and energy storage, are economically dispatched by a distribution system operator (DSO). A bi-level optimization model is formulated to guarantee the goals of both DSO and microgrids. It is solved by developing Karush-Kuhn-Tucker (KKT) conditions and combining the two problems into one mathematical programming with complementarity constraints (MPCC). Furthermore, since the physical topology and distribution power flow constraints are enclosed to form a non-convex optimal power flow (OPF) model, a convexification technique is implemented to transform the original problem into a mixed integer quadratic constrained problem (MIQCP) for better computation performance. At the transmission level, DSOs strategically bid with generation companies to win the desired share of the market managed by a transmission system operator (TSO). A multivariate linear regression (MLR) is developed to capture the correlation between the bid gained and the prices offered by the DSO and its opponents to maximize its possibility of winning the bid. Simulation studies on IEEE test systems verify the proposed framework.

Index Terms—Convexification, hierarchical balancing market, mathematical program with complementary constraints (MPCC), multi-microgrid, multivariate regression.

NOMENCLATURE

Acronyms:

DSR	Distributed sustainable resource
DR	Demand response
CHP	Combined heat and power plants
LSE	Load serving entity
PEV	Plug-in electric vehicle
DSO	Distribution system operator
DG	Distributed generator
MO	Market operator
MGA	Microgrid aggregator
WEM	Wholesale electricity market
LMP	Locational marginal price
RTBM	Real-time balancing market
MPCC	Mathematical program with complementary constraints
KKT	Karush-Kuhn-Tucker conditions
MIQCP	Mixed integer quadratic constrained programming
DLMP	Distribution locational marginal price

MLR	Multivariate linear regression
TSO	Transmission system operator
GENCO	Generation company
OPF	Optimal power flow
MG	Microgrid
PCC	Point of common coupling
QCP	Quadratic constrained programming
MPPT	Maximum power point tracking

Sets and Indices:

T	Index of the sub-hourly time interval
N_T	Length of sub-hourly time interval
t	Index within one sub-hourly time interval
k	Index of distributed generators
Z, z	Set and index of demand response block
m	Index of microgrids
i, j	Index of the head bus and tail bus of one line in the distribution/transmission system
N_{GENCO}, g	Set and index of generation companies at real-time balancing market
N_{DSO}	Set of distribution system operators at real-time balancing market

Constants:

a_k^p, b_k^p, c_k^p	Coefficients of generation cost function of the k^{th} distributed generator (DG)
$eC_m^z, q_m^z(t)$	Price and quantity of z^{th} demand response (DR) block in m^{th} microgrid [\$/MWh, MW]
$P_k^{DG, min}, P_k^{DG, max}$	Lower and upper generation bound of the k^{th} DG [MW]
$P_m^{Load}(t)$	Load of the m^{th} microgrid [MW]
$P_{es}^{ch, max}, P_{es}^{dis, max}$	Maximum charge/discharge rate of energy storage [MW]
$SOC_{es}^{min}, SOC_{es}^{max}$	Capacity limit of energy storage [MWh]
$P_m^{WT}(t), P_m^{PV}(t)$	Power generation of wind turbines and PVs in m^{th} microgrid [MW]
$\lambda^{pen}, \lambda^{loss}$	The price for power exchange deviation, and distribution network losses [\$/MWh]
r_{ij}, x_{ij}	Resistance and reactance of line ij at distribution system
y_{ij}	Admittance of line ij at distribution system
U^{min}, U^{max}	Bus voltage limit [p.u.]
$P_{j, DSO}^L(t), Q_{j, DSO}^L(t)$	Active/reactive load at bus j at distribution system [MW]
$P_{i, TSO, T}^L, Q_{i, TSO, T}^L$	Active/reactive load at bus i at transmission system [MW]

Y. Du and F. Li are with Department of EECS, The University of Tennessee, Knoxville, TN 37996. (Corresponding author: F. Li, email: fli6@utk.edu)

$a_{g,T}, b_{g,T}, c_{g,T}$	Generation cost coefficients of the g^{th} GENCO at T^{th} sub-hourly time interval
G_{ij}, B_{ij}	Conductance and susceptance of line ij at transmission system
P_d^{cap}	Maximum bidding capacity of DSO[MW]
$\lambda_{\text{GENCO},T}, P_{\text{GENCO},T}^{\text{bid}}$	Bidding price and bidding quantity of GENCOs at the T^{th} sub-hourly time interval [\$/MWh, MWh]
Variables:	
$C_{DG}^k(P_k^{\text{DG}}(t))$	Generation cost of the k^{th} DG [\$/MWh]
$P_k^{\text{DG}}(t)$	Generation of the k^{th} DG [MW]
$u_m^{\text{dr}}(t)$	0-1 binary variable of DR block
$P_{es}^{\text{ch}}(t), P_{es}^{\text{dis}}(t)$	Charge/discharge rate of energy storage [MW]
$EDR_m(t)$	The cost of dispatching DR in m^{th} microgrid [\$/MWh]
$SOCE_s(t)$	Energy level of energy storage [MWh]
$P_{m,\text{buy}}^{\text{grid}}(t), P_{m,\text{sell}}^{\text{grid}}(t)$	Power exchange between the m^{th} microgrid and the distribution system [MW]
$DR_m(t)$	The amount of DR dispatched in m^{th} microgrid [MW]
$\lambda_m(t)$	Distribution locational marginal price received by the m^{th} microgrid [\$/MWh]
$\delta P_{\text{PCC}}^{\text{RT}}(t)$	Deviation from scheduled power exchange at PCC[MW]
$P_{\text{PCC}}^{\text{RT}}(t)$	Real-time power exchange at PCC [MW]
$U_i(t), U_j(t)$	Head and tail bus voltage of line ij at distribution system [p.u.]
$P_{ij}^{\text{flow}}(t), Q_{ij}^{\text{flow}}(t)$	Active/reactive power flow on line ij at distribution system
$P_{ij}^{\text{loss}}(t), Q_{ij}^{\text{loss}}(t)$	Active/reactive power losses on line ij at distribution system
$I_{ij}(t)$	Current flow on line ij at distribution system
$P_{g,T}^G$	Generation quantity of the g^{th} GENCO at the T^{th} sub-hourly time interval [MWh]
$V_{i,T}, V_{j,T}$	Head and tail bus voltage of line ij at transmission system
$\theta_{ij,T}$	Voltage angle difference of line ij at transmission system
$\lambda_{\text{DSO},T}, P_{\text{DSO},T}^{\text{bid}}$	Bidding price and bidding quantity of DSO at the T^{th} sub-hourly time interval [\$/MWh, MWh]
$\lambda_{\text{DSO},T}^{\text{cleared}}, P_{\text{DSO},T}^{\text{cleared}}$	Market cleared price and cleared bid received by DSO at the T^{th} sub-hourly time interval [\$/MWh, MWh]

I. INTRODUCTION

THE emerging plug-and-play demand-side resources begin to take an non-negligible part in power system operation. Compared with conventional generators, these new distributed sustainable resources (DSRs), such as demand response (DR) programs, roof-top solar, electric vehicles or distributed energy storage, combined heat and power plants (CHP), hold the following benefits [1]: 1) they are free from ramping

insufficiency, which leads to faster response speeds; 2) the diversity of demand-side resources provides flexibility when reacting to a real-time dispatch schedule; 3) their dispersed distribution and closeness to end-consumers reduces long-distance power transfer losses. Therefore, it can be safely concluded that the various small-sized, elastic distributed sustainable resources possess considerable potentials in providing energy and ancillary services to the utility grid.

There are many studies focusing on involving demand response into transmission-level electricity market to improve market efficiency. Ref. [2] investigates the possible effects of load-shifting demand response program on market clearing, which suggests that a flexible shifting demand bid can contribute to both consumers' bill saving and total generation cost decreasing. Ref. [3]-[4] discuss the optimal dispatch schedule for load aggregator with multiple DR programs in wholesale electricity market, including load curtailment, load shifting, onsite generation, and energy storage. Ref. [5] explores leveraging direct load control in mitigating the risky variation of real-time critical peak pricing, where a multi-objective model is established to minimize both schedule cost and emission cost. Ref. [6] explores the possibility of exploiting demand-side reserve to support system reliability under $n-k$ contingency. A robust dispatch model is developed to optimize the total operation cost under worst-case contingency.

All the above works have established a solid foundation for further in-depth exploration of the significant potentials of demand-side sustainable resources in participating in electricity market and contributing to system-wide economy and stability improvement. The focus of these previous research works on the demand response performance are mainly at the transmission level. This applies to large-capacity industrial loads or large-scale aggregation of residential loads. However, for other small-scale demand-side resources such as distributed wind, roof-top solar, distributed energy storage (i.e., electric vehicle), diesel generation or fuel cell, direct penetration into transmission system is usually denied due to their limited capacity.

Furthermore, DSRs are usually located within several geographical regions, and their scattered penetration into the power system will result in mass organization, computation, and communication burdens, which limit the electricity market efficiency.

Motivated by the above two concerns, researchers have been working on developing a distribution-level electricity market to better aggregate various demand-side DSRs and to coordinate their operation with the bulk power system. In this regard, an intermediate party, i.e. a load serving entity (LSE) [7], a plug-in electric vehicle (PEV) aggregator [8], a microgrid aggregator [9], or a distribution system operator (DSO) [10], communicates with the upper-level utility grid and manages the economic operation of DSRs accordingly. A distribution-level electricity market framework is demonstrated in [11]-[12], where distributed generators (DGs), DRs, and microgrids trade with each other in the charge of a local electricity coordinator to maintain local power supply-demand balance. Dynamic pricing is formulated in [13] to stimulate microgrids to

exchange power with distribution networks. Ref. [14] inspects the effects of implementing distribution locational marginal price on different demand-side participants in contributing to distribution congestion management and voltage support. However, these studies focus on the participation of demand-side resources at the distribution level only, with no transmission system involved.

Refs. [15]-[16] model the interaction between distribution system with demand-side resources and transmission system. Further, these studies included uncertainties of the demand-side resources, which results in a two-stage problem. The price signals utilized by the distribution system operator to schedule demand-side resources are treated as constants. Ref. [17] considers the optimal bidding strategy for distribution company participating in both energy and reserve market. A multi-objective programming is designed in [18] to model the interactive behaviors among the transmission market operator (MO), DSO, and a network of microgrids with non-dispatchable renewable energy sources. In [19], a tri-level market framework is proposed to enable microgrids to participate in electricity market bidding through the microgrid aggregator (MGA). In [20]-[21], a more complex hierarchical market structure is proposed to include both wholesale electricity markets (WEMs) and distribution markets. For computation efficiency, the proposed tri-layer model is further transformed into bi-level programming by applying sensitivity functions and duality theory, respectively.

Inspired by the above works, a hierarchical real-time balancing market (RTBM) framework is proposed in this paper to stimulate DSR-driven microgrids to provide balancing service to the transmission system. The major novelty of our work, if compared with the previous works, is that we construct a tri-level electricity market mechanism with active DSRs' participation in real-time operation. The ramping-free feature and the diversity of DSRs gives it considerable flexibility in responding to real-time dispatch, hence making it an ideal alternative to conventional standby units for power regulation. To the best of the authors' knowledge, few studies have investigated the demand-side participation in tri-level interactive market at a real-time scale, which puts a higher requirement on computational efficiency, although the practicability of applying demand-side resources in day-ahead energy and reserve market has been deliberated in references [17]-[21].

Furthermore, each level of our model includes comprehensive market participants: in the local microgrid system, a variety of DSRs is comprised to demonstrate its flexibility; at the distribution system, physical constraints are encompassed to ensure the dispatch schedule is feasible in practice; and at the transmission system, the mutual relationship among different market participants is studied. Specifically, we design an optimal bidding strategy for each of DSOs with the consideration of interaction with other market participants, instead of simply transforming the multi-level program into one unified optimization problem with mathematics techniques. The model in the paper is more delicate and closer to real-world situations without much assumption and simplification.

The main technical contributions of this paper are detailed as follows:

- 1) At the distribution level of the proposed market framework, a bi-level model is formulated to optimize the goal of both distribution system operators and DSR-driven microgrid operators. It is later transformed into a mathematical program with complementarity constraints (MPCC) by developing Karush-Kuhn-Tucker (KKT) conditions for better computing efficiency.
- 2) The above MPCC model includes nonconvex distribution power flow constraints. A linearization technique is leveraged to reduce model complexity, which results in mixed integer quadratic constrained programming (MIQCP). The distribution locational marginal price (DLMP) is utilized as the control signal for the DSO to manage the individual microgrid's behaviors.
- 3) At the transmission level of the proposed market framework, DSO bids with other DSOs and generation companies in the balancing market to make up for the real-time power supply-demand gap of the transmission system. To maximize the probability of winning the bid, a multivariate linear regression (MLR) method is applied to study the correlation between the bid obtained and the price offered, which facilitates in the bidding decision making of the DSO.

The rest of this paper is organized as follows. Section II demonstrates the hierarchical real-time balancing market framework involving multiple microgrids; Section III models the interaction between the DSO and microgrids at the distribution level; Section IV formulates the transmission market bidding problem; Section V tests the proposed model on standard IEEE systems; and Section VI concludes the paper.

II. HIERARCHICAL REAL-TIME BALANCING MARKET FRAMEWORK WITH MULTI-MICROGRID PARTICIPATION

A. Market Framework

The real-time balancing market (RTBM) is part of the standard modern electricity market. The other parts include the day-ahead market and hour-ahead market. A RTBM is launched in each sub-hourly interval (e.g., 5-15 minutes) during the operational hour to clear any unbalance and to constantly guarantee systematic stability. This is realized by the transmission system operator (TSO) who selectively activates the bids submitted by generators with capacity resources or demand resources that are available to minimize system operation cost.

In this paper, we involve groups of DSR-driven microgrids in participating in RTBM bidding to provide balancing services to the transmission system under the management of the DSO. Since microgrids have no direct access to the transmission-level wholesale market, a hierarchical market framework is designed as shown in Fig. 1.

In Fig. 1 (a), the proposed market framework consists of two levels. At the transmission level market bidding, the participants include DSOs and generation companies (GENCOs), who submit their demand or generation blocks. The TSO then conducts an optimal power flow (OPF) calculation

and sends back the market clearing results to the bidders. At the distribution level, since the DSO does not own any power sources, it will stimulate the local microgrids (MGs) to reach the cleared market bid by releasing a price signal, i.e., the distribution locational marginal price (DLMP). An individual microgrid power exchange with a distribution system at the connected bus is obtained via an economic dispatch process under the given price. Finally, the aggregated response of multiple microgrids is evaluated as the power exchange at the point of common coupling (PCC), and should equal the cleared bid, as is demonstrated in Fig. 1 (b). In addition, we assume that a microgrid contains comprehensive DSRs including dispatchable generators (i.e. micro turbines, fuel cells, diesel generators), renewable generators (i.e. wind turbines, solar panels), energy storage, and demand response resources, which can also be observed from Fig. 1 (b).

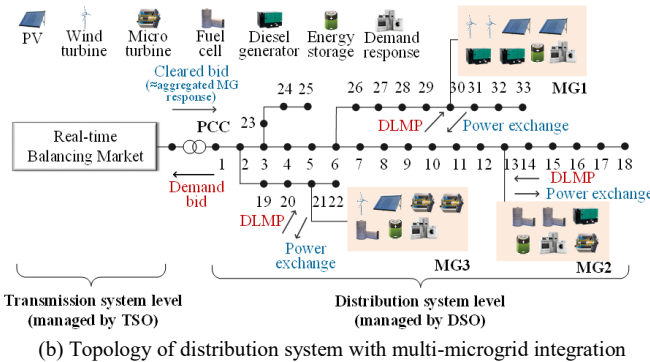
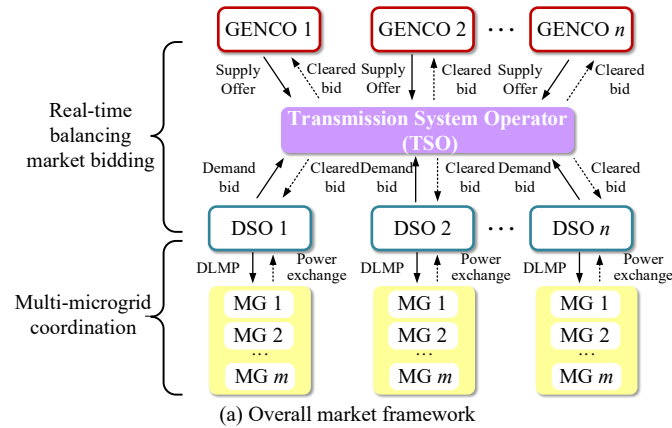
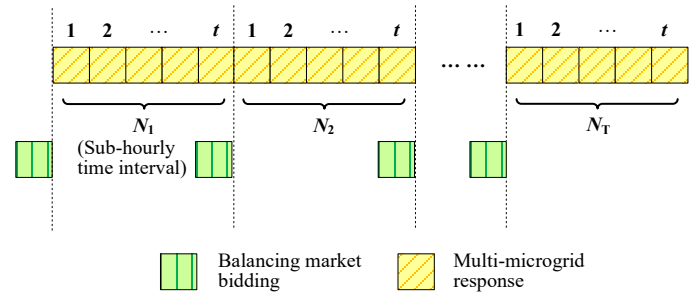


Fig. 1 Hierarchical real-time balancing market (RTBM) framework

The timeline of the proposed market is shown in Fig. 2. Note, from the figure, during real-time operation, one hour is split into several sub-hourly intervals with the same length. Before the starting of each sub-hourly time interval, the balancing market bidding will be launched, and DSO will receive the cleared bidding quantity and cleared price. Then, during the entire sub-hourly time interval, DSO will send out DLMP to microgrids to maintain the power exchange at the PCC to a steady level, i.e., the cleared bid.



B. Additional Remarks

According to ref. [22], the bidding blocks for the balancing market are submitted hours before the real-time operation. This applies to GENCOs in this paper. For DSOs, since their bidding blocks come from an aggregated microgrid response, which may fluctuate during real-time operation due to the existence of renewables and loads, we assume that DSOs can make modifications of their bidding blocks based on the latest forecast of the microgrid response for every sub-hourly time interval bidding. This decision-making process is accelerated by the convexification method that we utilize in the following section to meet with real-time dispatch.

Another remark concerns microgrid privacy. Generally, microgrid operators are autonomous entities who have the intact authority over local DSRs like DGs and demand. In our study, since microgrids have to depend on the DSO to participate in the electricity market, we assume that the DSO has certain access to microgrid information. This can be realized by ex-ante contracts between DSOs and microgrids. In the following work, we assume that the contract has already been formed and detailed discussion on this part is omitted.

III. DISTRIBUTION LEVEL PROBLEM FORMULATION: BI-LEVEL OPTIMIZATION

As stated in Section II-A, at the distribution level of the proposed hierarchical market framework, the DSO drives the microgrids to reach the cleared bid by utilizing DLMP. This is a bi-level optimization problem, since the DSO and microgrids have their respective objectives. Thus, one level for DSO and the other for microgrids are needed.

A. Lower-level Optimization: Economic Dispatch of Individual Microgrid

From the perspective of the microgrid operator, its optimal response under DLMP is derived from the following economic dispatch model:

$$\text{Min} \sum_{t=1}^{N_T} \left(\sum_{k \in m} C_{DG}^P(P_k^{DG}(t)) + \lambda_m(t) \times (P_{m,buy}^{grid}(t) - P_{m,sell}^{grid}(t)) + EDR_m(t) \right) \quad (1)$$

$$C_{DG}^P(P_k^{DG}(t)) = a_k^p + b_k^p P_k^{DG}(t) + c_k^p (P_k^{DG}(t))^2 \quad (2)$$

$$EDR_m(t) = \sum_{z=1}^Z e c_m^z q_m^z(t) u_m^z(t) \quad (3)$$

Eq. (1) calculates the operation cost of the m^{th} microgrid over one sub-hourly time interval, where the first term is the generation cost of dispatchable generators, which has a quadratic form, as shown in Eq. (2); the second term is the

power exchange cost, which is a product of DLMP, $\lambda_m(t)$ and the net power purchased by the microgrid. The last term is the cost of dispatching DR resources that reside in the microgrid, which is calculated by Eq. (3). $u_m^z(t)$ is a 0-1 binary variable indicating whether the z^{th} demand response block $q_m^z(t)$ is dispatched or not, and ec_m^z is the unit price. Microgrid economic dispatch should also satisfy the following constraints:

$$P_k^{DG,\min} \leq P_k^{DG}(t) \leq P_k^{DG,\max} \quad (4)$$

$$0 \leq DR_m(t) = \sum_{z=1}^Z q_m^z(t) u_m^z(t) \leq P_m^{\text{Load}}(t) \quad (5)$$

$$u_m^{z-1}(t) \geq u_m^z(t), \text{ for } z = 2, \dots, Z \quad (6)$$

$$0 \leq P_{es}^{ch}(t) \leq P_{es}^{ch,\max}, 0 \leq P_{es}^{dis}(t) \leq P_{es}^{dis,\max} \quad (7)$$

$$SOC_{es}(t) = SOC_{es}(t-1) + \eta_{es} P_{es}^{ch}(t) \Delta - P_{es}^{dis}(t) / \eta_{es} \Delta \quad (8)$$

$$SOC_{es}^{\min} \leq SOC_{es}(t) \leq SOC_{es}^{\max} \quad (9)$$

$$P_m^{\text{Load}}(t) - P_{m,\text{buy}}^{\text{grid}}(t) + P_{m,\text{sell}}^{\text{grid}}(t) - P_m^{\text{WT}}(t) - P_m^{\text{PV}}(t) - \sum_{k \in m} P_k^{DG}(t) - \sum_{es \in m} (P_{es}^{dis}(t) - P_{es}^{ch}(t)) - DR_m(t) = 0 \quad (10)$$

Eq. (4) is the generator capacity constraint of DGs in the m^{th} microgrid; Eqs. (5)-(6) limit that the total demand response dispatched should not exceed the load, and the demand response blocks are dispatched in an increasing order; Eq. (7) is the charge/discharge rate limit of the energy storage; Eq. (8) calculates the energy level of energy storage, where η_{es} is its efficiency and Δ is the length of the time interval; Eq. (9) is the capacity limit of energy storage; finally, Eq. (10) is the power balance constraint of the microgrid.

In the above microgrid economic dispatch model, the network losses are not included in the power balance constraint. The reason is that in our model, microgrids are connected to the main distribution system. The network losses of the small-scale microgrid are negligible if compared with the distribution network losses (i.e., the power losses along the main feeder). Furthermore, the model is designed for a real-time application, which requires fast computational speed. Hence, for model simplicity and computational efficiency, the power loss of microgrid in the lower-level economic dispatch is neglected.

Note that in the objective function (1), the second term is nonconvex, since the DLMP received by the m^{th} microgrid is unknown until DSO calculates an optimal power flow. We will later address this issue by applying KKT conditions at the end in this section.

B. Upper-level Optimization: Minimizing Power Exchange Deviation

From the perspective of DSO, the real-time power exchange that takes place at PCC should equal the cleared bid at the balancing market. The DSO solves the following optimization problem with the aim of minimizing the deviation of actual power flow at PCC from the cleared bid:

$$\text{Min} \sum_{t=1}^{N_T} (\lambda^{\text{pen}} \delta P_{PCC}^{\text{RT}}(t) + \sum_{ij} \lambda^{\text{loss}} P_{ij}^{\text{loss}}(t)) \quad (11)$$

$$P_{PCC}^{\text{RT}}(t) = \sum_{i=1} P_{ij}^{\text{flow}}(t) \quad (12)$$

$$\delta P_{PCC}^{\text{RT}}(t) \geq P_{DSO,T}^{\text{cleared}} - P_{PCC}^{\text{RT}}(t), \delta P_{PCC}^{\text{RT}}(t) \geq -P_{DSO,T}^{\text{cleared}} + P_{PCC}^{\text{RT}}(t) \quad (13)$$

$$0 \leq \delta P_{PCC}^{\text{RT}}(t) \leq \alpha P_{DSO,T}^{\text{cleared}} \quad (14)$$

$$P_{ij}^{\text{flow}}(t) - \sum_{j' \in n(j)} P_{jj'}^{\text{flow}}(t) - P_{ij}^{\text{loss}}(t) = P_{j,DSO}^L(t) - \sum_{m \in j} (P_{m,\text{sell}}^{\text{grid}}(t) - P_{m,\text{buy}}^{\text{grid}}(t)) \quad (15)$$

$$Q_{ij}^{\text{flow}}(t) - \sum_{j' \in n(j)} Q_{jj'}^{\text{flow}}(t) - Q_{ij}^{\text{loss}}(t) = Q_{j,DSO}^L(t) \quad (16)$$

$$P_{ij}^{\text{loss}}(t) = ((\text{Re}\{U_i(t)\} - \text{Re}\{U_j(t)\})^2 + (\text{Im}\{U_i(t)\} - \text{Im}\{U_j(t)\})^2) * \text{Re}\{y_{ij}^*\} \quad (17)$$

$$Q_{ij}^{\text{loss}}(t) = ((\text{Re}\{U_i(t)\} - \text{Re}\{U_j(t)\})^2 + (\text{Im}\{U_i(t)\} - \text{Im}\{U_j(t)\})^2) * \text{Im}\{y_{ij}^*\} \quad (18)$$

$$\text{Re}\{U_j(t)\} = |U_i(t)| - \frac{(P_{ij}^{\text{flow}}(t)r_{ij} + Q_{ij}^{\text{flow}}(t)x_{ij})}{|U_i(t)|} \quad (19)$$

$$\text{Im}\{U_j(t)\} = -\frac{(P_{ij}^{\text{flow}}(t)x_{ij} - Q_{ij}^{\text{flow}}(t)r_{ij})}{|U_i(t)|} \quad (20)$$

$$|U_i(t)| = \sqrt{(\text{Re}\{U_i(t)\})^2 + (\text{Im}\{U_i(t)\})^2} \quad (21)$$

$$U^{\min} \leq \text{Re}\{U_i(t)\} \leq U^{\max} \quad (22)$$

In Eq. (11), the first two terms are the penalty for deviating from the market cleared bid and network losses cost, where λ^{pen} and λ^{loss} are the price for power deviation and losses, and $\delta P_{PCC}^{\text{RT}}$ is the power exchange deviation. Note, the reason for minimizing the power exchange deviation is that the DSO first bids in the transmission-level balancing market and receives a cleared quantity. Then, it drives the microgrids to reach the cleared quantity required by the transmission system via price incentive; otherwise DSO will be penalized by the transmission market. The cleared quantity is measured as the power exchange at the PCC. As a result, the DSO includes the deviation of actual power exchange at PCC from the cleared quantity in its objective function to minimize the potential penalty.

Eq. (12) calculates the real-time power exchange at PCC. The power deviation is calculated by Eq. (13) to guarantee that the penalty is always positive, where $P_{DSO,T}^{\text{cleared}}$ is the market cleared bid received by DSO at the T^{th} sub-hourly time interval. Eq. (14) ensures that the deviation is confined within a certain bound; in the following simulations, α is set to 1%. Eq. (15)-(16) are the power flow constraints in the DistFlow form, where $n(j)$ is the set of buses that belong to the line with bus j as the head bus. Eq. (17)-(18) calculate the active and reactive losses on line ij . A detailed deduction of the line loss calculations is shown as follows [23]:

$$\begin{aligned} P_{ij}^{\text{loss}}(t) &= \text{Re}\{U_i(t)I_{ij}^*(t)\} - \text{Re}\{U_j(t)I_{ij}^*(t)\} \\ &= \text{Re}\{U_i(t)(U_i^*(t) - U_j^*(t)) - U_j(t)(U_i^*(t) - U_j^*(t))\} * \text{Re}\{y_{ij}^*\} \\ &= \text{Re}\{e_i^2 + f_i^2 - 2e_i e_j - 2f_i f_j + e_j^2 + f_j^2\} * \text{Re}\{y_{ij}^*\} \\ &= \text{Re}\{(e_i - e_j)^2 + (f_i - f_j)^2\} * \text{Re}\{y_{ij}^*\} = \text{Eq.}(17) \end{aligned} \quad (23)$$

The same applies to the reactive line loss calculation. Eq. (19)-(20) calculate the bus voltage magnitude of line ij . It can be noticed that both constraints are nonconvex due to the existence of division. For the sake of simplicity, we assume that in distribution system, the bus voltage magnitude is around 1 p.u. i.e. $|U_i(t)| \approx 1$; and the bus voltage angle is around 0 rad, i.e.

$\text{Im}\{U_i(t)\} \approx 0$, $|U_i(t)| \approx \text{Re}\{U_i(t)\}$. Hence, Eq. (19)-(20) can be rewritten as:

$$\text{Re}\{U_j(t)\} = \text{Re}\{U_i(t)\} - (P_{ij}^{\text{flow}}(t)r_{ij} + Q_{ij}^{\text{flow}}(t)x_{ij}) \quad (24)$$

$$\text{Im}\{U_j(t)\} = -(P_{ij}^{\text{flow}}(t)x_{ij} - Q_{ij}^{\text{flow}}(t)r_{ij}) \quad (25)$$

The above linearization leads to quadratic constrained programming (QCP), which can be directly cracked by existing solvers. Eq. (22) is the boundary of voltage magnitude, in this case it is set to [0.95 p.u., 1.05 p.u.].

C. Reconstruction of the Bi-level Optimization into MPCC

As is shown above, at the distribution level, both the DSO and microgrids have their own objective functions and operation constraints, which is a bi-level problem. For efficient computation, we apply KKT (Karush-Kuhn-Tucker) conditions of the microgrid economic dispatch problem and transform the bi-level problem into the following mathematical programming with complementarity constraint (MPCC):

First, we introduce Lagrangian multipliers to constraints (4)-(10) and acquire the following Lagrangian function:

$$\begin{aligned} L_m = & \sum_{t=1}^{N_T} \left(\sum_{k \in m} (C_{DG}^P(P_k^{DG}(t))) + \lambda_m(t) \times (P_{m,\text{buy}}^{\text{grid}}(t) - P_{m,\text{sell}}^{\text{grid}}(t)) + \text{EDR}_m(t) \right. \\ & + \sum_{k \in m} (\omega_k^{\min}(t)(P_k^{DG,\min}(t) - P_k^{DG}(t)) + \omega_k^{\max}(t)(P_k^{DG}(t) - P_k^{DG,\max}(t))) \\ & + \sum_{z=2}^Z \omega_m^z(t)(u_m^z(t) - u_m^{z-1}(t)) + \omega_m^{\min}(t)(0 - \sum_{z=1}^Z q_m^z(t)u_m^z(t)) \\ & + \omega_m^{\max}(t)(\sum_{z=1}^Z q_m^z(t)u_m^z(t) - P_m^{\text{load}}(t)) \\ & + \sum_{es \in m} (\omega_{es}^{\text{ch},\min}(t)(0 - P_{es}^{\text{ch}}(t)) + \omega_{es}^{\text{ch},\max}(t)(P_{es}^{\text{ch}}(t) - P_{es}^{\text{ch},\max})) \\ & + \omega_{es}^{\text{dis},\min}(t)(0 - P_{es}^{\text{dis}}(t)) + \omega_{es}^{\text{dis},\max}(t)(P_{es}^{\text{dis}}(t) - P_{es}^{\text{dis},\max}) \\ & + \omega_{es}^{\text{soc},\min}(t)(\text{SOC}_{es}^{\min} - \text{SOC}_{es}(t)) + \omega_{es}^{\text{soc},\max}(t)(\text{SOC}_{es}(t) - \text{SOC}_{es}^{\max}) \\ & + v_{es}(t)(\text{SOC}_{es}(t) - \text{SOC}_{es}(t-1) - \eta_{es} P_{es}^{\text{ch}}(t)\Delta + P_{es}^{\text{dis}}(t) / \eta_{es}\Delta) \\ & + v_m(t)(P_m^{\text{load}}(t) - P_{m,\text{buy}}^{\text{grid}}(t) + P_{m,\text{sell}}^{\text{grid}}(t) - P_m^{\text{PV}}(t) - \sum_{k \in m} P_k^{DG}(t) \\ & - \sum_{es \in m} (P_{es}^{\text{dis}}(t) - P_{es}^{\text{ch}}(t)) - \text{DR}_m(t) \end{aligned} \quad (26)$$

In Eq. (26), $\omega_k^{\min}(t)$, $\omega_k^{\max}(t)$, $\omega_m^z(t)$, $\omega_m^{\min}(t)$, $\omega_m^{\max}(t)$, $\omega_{es}^{\text{ch},\min}(t)$, $\omega_{es}^{\text{ch},\max}(t)$, $\omega_{es}^{\text{dis},\min}(t)$, $\omega_{es}^{\text{dis},\max}(t)$, $\omega_{es}^{\text{soc},\min}(t)$, $\omega_{es}^{\text{soc},\max}(t)$, $v_{es}(t)$, and $v_m(t)$ are the Lagrangian multiplier for the constraints (4)-(10), respectively. We further develop the following KKT conditions, including 1st order partial derivatives and complementary slackness constraints, as an equivalent alternative of the microgrid economic dispatch model:

1) 1st order partial derivative:

$$\nabla L_m |_{P_k^{DG}(t)} = 0 \Rightarrow 2c_k^p P_k^{DG}(t) + b_k^p - \omega_k^{\min}(t) + \omega_k^{\max}(t) - v_m(t) = 0 \quad (27)$$

$$\nabla L_m |_{P_{m,\text{buy}}^{\text{grid}}(t)} = 0 \Rightarrow \lambda_m(t) - v_m(t) = 0 \quad (28)$$

$$\nabla L_m |_{P_{m,\text{sell}}^{\text{grid}}(t)} = 0 \Rightarrow -\lambda_m(t) + v_m(t) = 0$$

$$\begin{aligned} \nabla L_m |_{u_m^z(t)} = 0 \Rightarrow & ec_m^z q_m^z(t) + \omega_m^z(t) - \omega_m^{z+1}(t) - \omega_m^{\min}(t) q_m^z(t) \\ & + \omega_m^{\max}(t) q_m^z(t) - v_m(t) q_m^z(t) = 0, \quad z = 1, \dots, Z-1 \end{aligned} \quad (29)$$

$$\begin{aligned} \nabla L_m |_{q_m^z(t)} = 0 \Rightarrow & ec_m^z q_m^z(t) + \omega_m^z(t) - \omega_m^{\min}(t) q_m^z(t) \\ & + \omega_m^{\max}(t) q_m^z(t) - v_m(t) q_m^z(t) = 0, \quad z = Z \end{aligned} \quad (30)$$

$$\nabla L_m |_{P_{es}^{\text{ch}}(t)} = 0 \Rightarrow -\omega_{es}^{\text{ch},\min}(t) + \omega_{es}^{\text{ch},\max}(t) - v_{es}(t)\eta_{es}\Delta + v_m(t) = 0$$

$$\nabla L_m |_{P_{es}^{\text{dis}}(t)} = 0 \Rightarrow -\omega_{es}^{\text{dis},\min}(t) + \omega_{es}^{\text{dis},\max}(t) + v_{es}(t) / \eta_{es}\Delta - v_m(t) = 0 \quad (31)$$

$$\begin{aligned} \nabla L_m |_{\text{SOC}_{es}(t)} = 0 \Rightarrow & -\omega_{es}^{\text{SOC},\min}(t) + \omega_{es}^{\text{SOC},\max}(t) \\ & + v_{es}(t)\Delta - v_{es}(t+1)\Delta = 0, \quad t = 1, \dots, N_T - 1 \end{aligned} \quad (32)$$

$$\begin{aligned} \nabla L_m |_{\text{SOC}_{es}(t)} = 0 \Rightarrow & -\omega_{es}^{\text{SOC},\min}(t) + \omega_{es}^{\text{SOC},\max}(t) \\ & + v_{es}(t)\Delta = 0, \quad t = N_T \end{aligned} \quad (33)$$

2) Complementary slackness:

$$0 \leq \omega_k^{\min}(t) \perp (P_k^{DG}(t) - P_k^{DG,\min}) \geq 0 \quad (34)$$

$$0 \leq \omega_k^{\max}(t) \perp (P_k^{DG,\max} - P_k^{DG}(t)) \geq 0$$

$$0 \leq \omega_m^{\min}(t) \perp \sum_{z=1}^Z q_m^z(t)u_m^z(t) \geq 0 \quad (35)$$

$$0 \leq \omega_m^{\max}(t) \perp (P_m^{\text{load}}(t) - \sum_{z=1}^Z q_m^z(t)u_m^z(t)) \geq 0$$

$$0 \leq \omega_m^z(t) \perp u_m^{z-1}(t) - u_m^z(t) \geq 0 \quad (36)$$

$$0 \leq \omega_{es}^{\text{ch},\min}(t) \perp P_{es}^{\text{ch}}(t) \geq 0 \quad (37)$$

$$0 \leq \omega_{es}^{\text{ch},\max}(t) \perp (P_{es}^{\text{ch},\max} - P_{es}^{\text{ch}}(t)) \geq 0$$

$$0 \leq \omega_{es}^{\text{dis},\min}(t) \perp P_{es}^{\text{dis}}(t) \geq 0 \quad (38)$$

$$0 \leq \omega_{es}^{\text{dis},\max}(t) \perp (P_{es}^{\text{dis},\max} - P_{es}^{\text{dis}}(t)) \geq 0$$

$$0 \leq \omega_{es}^{\text{soc},\min}(t) \perp (\text{SOC}_{es}(t) - \text{SOC}_{es}^{\min}) \geq 0 \quad (39)$$

$$0 \leq \omega_{es}^{\text{soc},\max}(t) \perp (\text{SOC}_{es}^{\max} - \text{SOC}_{es}(t)) \geq 0$$

$$0 \leq P_{es}^{\text{dis}}(t) \perp P_{es}^{\text{ch}}(t) \geq 0 \quad (40)$$

$$0 \leq P_{m,\text{buy}}^{\text{grid}}(t) \perp P_{m,\text{sell}}^{\text{grid}}(t) \geq 0 \quad (41)$$

3) Equality constraints (8),(10);

Eq. (27)-Eq. (41) are the equivalent representation of the individual microgrid economic dispatch problem (1)-(10). The first-order partial derivative of each variable to the Lagrangian function (26) is calculated and is set to zero to constitute equality constraints. This is because at the optimal point, the first-order partial derivative should be zero. The above functions are Eq. (27)–Eq. (33). Next, the inequality constraints in the original economic dispatch model are represented by complementary slackness constraints, as is shown by Eq. (34)–Eq. (39). The complementary slackness constraint means that the product of the Lagrangian multiplier and the inequality constraint should be zero. Complementary slackness is an indicator of whether the original constraint is active or not. If the original constraint is strictly “less than”, then the Lagrangian multiplier is zero; if the Lagrangian multiplier is greater than zero, then the inequality should equal 0, meaning that the variable reaches the boundary. Eq. (40) indicates that the charge and discharge of energy storage cannot happen in the same time. Eq. (41) indicates that the buying and selling of microgrid power also cannot happen in the same time.

From Eq. (28), we can see that the original nonconvex term $\lambda_m(t) \times (P_{m,\text{buy}}^{\text{grid}}(t) - P_{m,\text{sell}}^{\text{grid}}(t))$ in the microgrid objective function (1) is decoupled into a linear equality constraint. The DLMP received by the microgrid equals the Lagrangian multiplier of the power balance constraint $v_m(t)$. $v_m(t)$ also appears in Eq. (27), (29) and (31), which can be explained as the marginal cost for power sources in the microgrid should equal the compensation, i.e., DLMP.

Note that in the complementary slackness constraints, there still exists a nonconvex term, which is the product of two variables, e.g. $\omega_k^{\min}(t) P_k^{DG}(t)$. We apply the big-M method to linearize the constraint as follows:

$$\begin{aligned}
 0 &\leq \omega_k^{\min}(t) \perp (P_k^{DG}(t) - P_k^{DG,\min}) \geq 0 \\
 \Rightarrow 0 &\leq P_k^{DG}(t) - P_k^{DG,\min} \leq M \cdot \delta_k^{\min}(t) \\
 0 &\leq \omega_k^{\min}(t) \leq M \cdot (1 - \delta_k^{\min}(t)), \delta_k^{\min}(t) \in \{0,1\}
 \end{aligned} \quad (42)$$

In Eq. (42), M is a very large number and $\delta_k^{\min}(t)$ is a 0-1 binary variable. This transformation can be uniformly applied to Eq. (34)-(41). By now, the lower level microgrid ED problem is replaced by the above affine constraints with binary variables. These constraints are added to the QCP model of the DSO, which eventually leads to the following MPCC problem: minimizing (11), subject to (8),(10),(12)-(18), (22),(24)-(25), (27)-(41), which is in essence a mixed integer quadratic constrained programming (MIQCP).

IV. TRANSMISSION LEVEL PROBLEM FORMULATION: STRATEGIC MARKET BIDDING

A. Balancing Market Bidding: an ACOPF Problem

As stated in Section II-A, at the transmission-level balancing market, DSOs and GENCOs submit their bidding blocks. The bidding blocks follow a staircase fashion for marginal cost (i.e., piece-wise-linear for the total cost curve).

The bidding blocks of GENCOs include the generation quantity and the desired price; the bidding blocks of DSOs include the demand quantity and the price they are willing to offer. After the TSO receives all the bidding blocks, it will first convert the bidding blocks into corresponding generator capacities and costs (demand bids are treated as negative generation), then runs the following ACOPF to find the optimal generator allocation and the locational marginal price:

$$\min \sum_{g=1}^{N_{GENCO}} (a_{g,T} (P_{g,T}^G)^2 + b_{g,T} P_{g,T}^G + c_{g,T}) + \sum_{d=1}^{N_{DSO}} (-\lambda_{DSO,T}) P_{DSO,T}^{bid} \quad (43)$$

$$\begin{aligned}
 s.t. \quad &\sum_{g \in i} P_{g,T}^G - P_{i,TSO,T}^L - \sum_{DSO \in i} P_{DSO,T}^{bid} \\
 &= V_{i,T} \sum_{j=1}^n V_{j,T} (G_{ij} \cos \theta_{ij,T} + B_{ij} \sin \theta_{ij,T}) \quad (44)
 \end{aligned}$$

$$-Q_{i,TSO,T}^L = V_{i,T} \sum_{j=1}^n V_{j,T} (G_{ij} \sin \theta_{ij,T} - B_{ij} \cos \theta_{ij,T}) \quad (45)$$

$$P_{g,T}^{G,\min} \leq P_{g,T}^G \leq P_{g,T}^{G,\max}, 0 \leq P_{DSO,T}^{bid} \leq P_d^{cap} \quad (46)$$

In Eq. (43), $a_{g,T}$, $b_{g,T}$ and $c_{g,T}$ are the generation cost coefficients of the g^{th} GENCO at T^{th} sub-hourly time interval (transformed from the staircase bidding curves); $P_{g,T}^G$ is the generation quantity; $\lambda_{DSO,T}$ is the price offered by the d^{th} DSO; and $P_{DSO,T}^{bid}$ is its demand. N_{GENCO} and N_{DSO} are the total number of generation companies and DSOs participating in market bidding, respectively. Eqs. (44)-(45) are the power balance constraints at the transmission system. Eq. (46) represents the upper and lower bounds of generation and demand, which can be obtained from their bidding blocks. After solving the above ACOPF, the TSO converts the generator allocation and price into cleared bids and notices the bidders. The uniform price equal to the marginal unit price is set as the price settlement rule. The above process repeats for every sub-hourly time interval until reaching the end of 1 hour.

In our study, we assume that GENCOs submit a set of supply offers containing three bidding blocks, and DSOs submit a set

of demand bids containing one bidding block. Neither GENCOs nor DSOs have the knowledge of the bidding blocks of their counterparts, therefore it's an incomplete information decision-making process for DSOs to form bidding blocks. To win the desired bid, we apply multivariate linear regression in the next part to optimize the DSO's bidding strategies.

B. Strategic Bidding based on MLR

The aim of strategic bidding for DSOs is to find the optimal price to offer in the market to gain the desired amount of power. According to the market rules, the demand block with the highest price will be first activated by TSO. On the other hand, the DSO intends to lower the price as much as possible to save the cost for purchasing power. To balance the trade-off between winning the bid and lowering the price, one effective way is to study the relationship between the bidding price and the cleared quantity. In this part, we apply a multivariate linear regression (MLR) method to describe this specific relationship.

It can be deduced from Eq. (43)-(46) that the cleared bid of one DSO is affected by the generation quantity and the associated price of GENCOs, as well as the demand bid of other DSOs, hence can be expressed as follows:

$$P_{DSO,T}^{cleared} = f(\lambda_{GENCO,T}, \lambda_{DSO,T}, \tilde{\lambda}_{DSO,T}, \mathbf{P}_{GENCO,T}^{bid}, \mathbf{P}_{DSO,T}^{bid}, \mathbf{P}_{DSO,T}^{bid}) \quad (47)$$

In Eq. (47), the first three terms in function f are the bidding prices of GENCOs, the DSO, and other DSOs at the T^{th} sub-hourly time interval, the fourth term is the bidding quantity of GENCOs, and the last two terms are the bidding quantity of the DSO and other DSOs. The letter in bold represents the vector. For simplicity, we assume that GENCOs have a large enough capacity to support the demand of all DSOs, and the marginal cost of GENCOs is lower than the price offered by DSO. Hence $\lambda_{GENCO,T}$, $\mathbf{P}_{GENCO,T}^{bid}$ (both are $1 \times N_{GENCO}$ vectors), $P_{DSO,T}^{bid}$, and $\mathbf{P}_{DSO,T}^{bid}$ (both are $1 \times (N_{DSO}-1)$ vectors) can be neglected in function f . A multivariate linear function can be developed as follows to calculate the bidding price:

$$\begin{aligned}
 P_{DSO,T}^{cleared} &= f(\lambda_{DSO,T}, \tilde{\lambda}_{DSO,T}) \Rightarrow \\
 \lambda_{DSO,T} &= [\mathbf{W}_{DSO,T}^*, \mathbf{W}_{DSO,T}^{cleared}] [\tilde{\lambda}_{DSO,T}, P_{DSO,T}^{cleared}]^T \quad (48)
 \end{aligned}$$

Notice that in Eq. (48), $\mathbf{W}_{DSO,T}^*$ is a $1 \times (N_{DSO}-1)$ coefficient vector of $\tilde{\lambda}_{DSO,T}$, and $\mathbf{W}_{DSO,T}^{cleared}$ is the coefficient of $P_{DSO,T}^{cleared}$. The above multivariate regression process relies on the historical bidding data to obtain the accurate coefficients.

The overall balancing market bidding process is depicted in Fig. 3, and is summarized as follows:

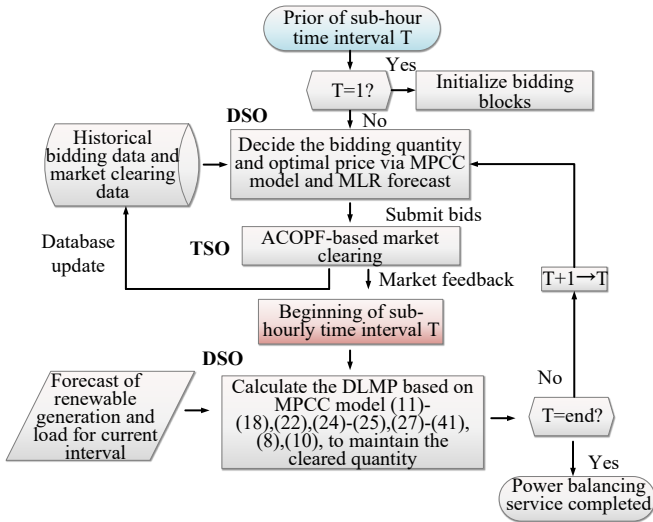


Fig. 3. Hierarchical balancing market bidding process

1) Prior to the beginning of sub-hourly time interval T , the real-time balancing market bidding is launched at the transmission level. DSOs decide their optimal bidding quantity and bidding price based on the following MPCC model:

$$\text{Min} \sum_{t=1}^{N_T} (\lambda_{DSO,T-1}^{\text{cleared}} P_{PCC}^{\text{RT}}(t) + \sum_{ij} \lambda_{ij}^{\text{loss}} P_{ij}^{\text{loss}}(t)) \quad (49)$$

$$s. t. (8), (10), (12) - (18), (22), (24) - (25), (27) - (41)$$

$$P_{DSO,T}^{\text{bid}} = \sum_{t=1}^{N_T} P_{PCC}^{\text{RT}}(t) / N_T \quad (50)$$

Note that Eq. (49) is slightly different from Eq. (11) in the first term. The former is $\lambda_{DSO,T-1}^{\text{cleared}} P_{PCC}^{\text{RT}}(t)$, while the latter is $\lambda^{\text{pen}} \delta P_{PCC}^{\text{RT}}$. The reason is that, to calculate the bidding quantity at the T^{th} sub-hourly time interval, $P_{DSO,T}^{\text{bid}}$, we first need to calculate the assumptive power exchange at PCC, $P_{PCC}^{\text{RT}}(t)$, at the T^{th} interval. This value is obtained by running the dispatch under the price stimulus of $\lambda_{DSO,T-1}^{\text{cleared}}$, which is the market clearing price at the $(T-1)^{\text{th}}$ interval. Then $P_{PCC}^{\text{RT}}(t)$ is averaged over N_T to obtain $P_{DSO,T}^{\text{bid}}$. Since the bidding starts at the beginning of the T^{th} time interval, and the DSO has no knowledge of the upcoming load and RES generation in the microgrids, therefore cannot be certain of the exact amount of power exchange that will take place at PCC. By averaging the power exchange as the bidding quantity, the real-time deviation can be minimized. After getting the value of $P_{DSO,T}^{\text{bid}}$, it is placed in Eq. (48) to get $\lambda_{DSO,T}^{\text{cleared}}$ (set $P_{DSO,T}^{\text{cleared}} = P_{DSO,T}^{\text{bid}}$) via MLR, and therefore, $P_{DSO,T}^{\text{bid}}$ and $\lambda_{DSO,T}^{\text{cleared}}$ constitutes the bidding block for the T^{th} sub-hourly time interval $(\lambda_{DSO,T}^{\text{cleared}}, P_{DSO,T}^{\text{bid}})$.

2) DSOs submit the customized bidding blocks to the balancing market, and then obtain the market clearing price and cleared quantity from TSO. The historical record is updated based on the latest market clearing result to improve the accuracy of MLR analysis.

3) At the beginning of the T^{th} sub-hourly time interval, DSO decides the DLMP based on MPCC model (11), and motivates the local microgrids to generate the required cleared quantity at PCC. The uncertain factors, i.e., renewable generation and load consumption, are updated based on the latest forecast.

4) If the whole market process does not reach the end of the operation period, then goes to 1) to repeat the above steps. Otherwise the power balancing service is completed.

From Section III and Section IV, note that in the proposed tri-level market model, microgrids with multiple DSRs are treated as price takers, since they respond to the DLMP released by the DSO; and DSO is regarded as price makers at the transmission-level market bidding. This role-setting is reasonable since the aggregation of large number of microgrids increases the market power of DSO and makes it possible for DSO to negotiate at the transmission bidding market, which can prevent oligopoly and eventually improve market efficiency.

V. CASE STUDY

A. Test case description and modeling parameters

In this section we test the proposed hierarchical market framework on the IEEE 30-bus system, which is served as the balancing market. Six GENCOs and three DSOs participate in market bidding. The IEEE 33-bus distribution system, IEEE 13-bus distribution system, and IEEE 69-bus distribution system serve as DSOs. Three microgrids are connected to the IEEE 33-bus distribution system, as shown in Fig. 1 (b). The 13-bus system has 2 microgrids connected, and the 69-bus system has 5 microgrids connected. The compositions of each microgrid are summarized in TABLE I. The parameters for various Distributed Sustainable Resources (DSRs) such as distributed wind turbine (WT), solar photovoltaic (PV), diesel generation (DE), micro turbine (MT), fuel cell (FC), energy storage (ES), and demand response (DR) are obtained from [24]-[25]. Also, WT, PV, DE, MT and FC are referred to as DGs in the case study. Wind turbines and PVs are assumed to work at MPPT (maximum power point tracking) mode with zero cost. Wind speed data, solar irradiation data and load data are obtained from [26]-[27].

TABLE I MICROGRID COMPOSITION

DSO1	MG1: WT, WT, PV, PV, DE, DE, ES, DR	MG2: DE, MT, FC, ES, DR
	MG3: WT, PV, MT, MT, FC, ES, DR	
DSO2	MG1: WT, WT, PV, MT, MT, ES, DR	MG2: WT, FC, FC, DR
DSO3	MG1: WT, PV, PV, DE, DE, ES, DR	MG2: WT, DE, MT, ES, DR
	MG3: WT, PV, MT, MT, ES, DR	MG4: WT, FC, FC, FC, ES, DR
	MG5: PV, WT, FC, DR	

WT: wind turbine; PV: photovoltaic panel; DE: diesel generation; MT: micro turbine; FC: fuel cell; ES: energy storage; DR: demand response

B. Simulation results

(1) Verification of quadratic-constrained power flow model

In our simulation, we first test the accuracy of the applied quadratic constrained power flow model (15)-(18), (24)-(25). We compare the bus voltage results between a standard AC power flow calculation and QCP calculation. The maximum relative error of bus voltage for a 13-bus system, 33-bus system, and 69-bus system are 0.005%, 0.383%, and 0.437%. The comparison verifies that the simplified QCP power flow model is an accurate enough substitute of AC power flow model.

Furthermore, since the proposed hierarchical market framework is set in a real-time context, the computation performance is a significant concern, and is illustrated as follows: the simulation is carried out on a hybrid platform, MATLAB 2016a and GAMS 24.7. The transmission-level balancing market bidding is completed by Matpower/Smart

Market [28]. The distribution level MIQCP problem is solved by DICOPT on GAMS. The hardware environment is a laptop with Intel®Core™ i5-6300U 2.4 GHz CPU, and 4.00 GB RAM. For the 13-bus system, the number of equations is 851, and the number of variables is 801, including 135 integer variables; for the 33-bus system, the number of equations is 2,096, and the number of variables is 2001, including 270 integer variables; for the 69-bus system, the number of equations is 3851, and the number of variables is 3726, including 390 integer variables. Computation time for deriving the DLMP in each sub-hourly interval is provided in TABLE II:

TABLE II COMPUTATION EFFICIENCY OF MIQCP MODEL FOR DSOs

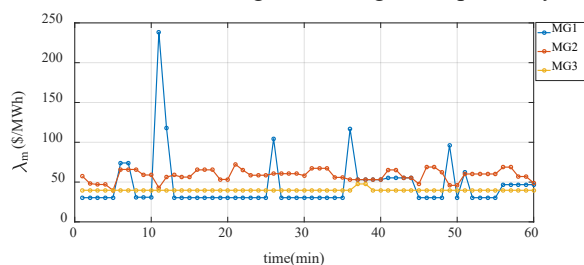
Interval index	1	2	3	4	5	6	7	8	9	10	11	12
DSO1	0.99	1.73	1.36	1.84	2.15	1.29	1.43	0.99	1.22	1.14	1.64	1.00
DSO2	0.46	0.47	0.49	0.37	0.46	0.62	0.59	0.44	0.53	0.42	0.48	0.56
DSO3	1.78	1.64	2.38	1.79	3.01	2.45	2.33	1.70	2.40	1.71	1.67	1.75

The longest computation time is 3.01 seconds. Since the market bidding process takes place before the sub-hourly time interval begins, and each sub-hourly time interval is 5 minutes, this computation time is fast enough for real-time dispatch.

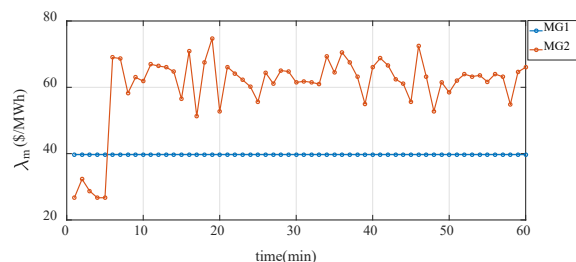
On the other hand, if the original power flow constraints (19)–(21) are directly applied in the MPCC model of DSO, the solver cannot find the solutions that satisfy all the constraints within the given time limit due to the nonconvexity of the constraints. Hence, the proposed MIQCP method is both reasonable and necessary for such a real-time application case.

(2) DLMP and microgrid response

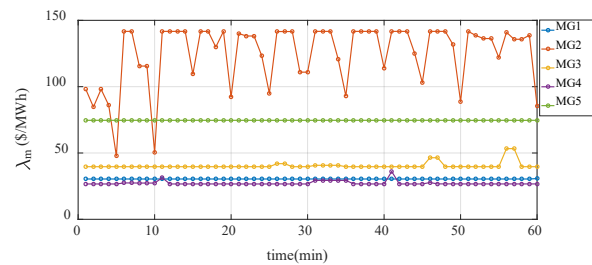
The simulation span is set to one hour, and it's evenly divided into 12 sub-hourly time intervals. The DLMP based on the MPCC model (11) for three DSOs and the associated DG generations are shown in Fig. 4. and Fig. 5, respectively:



(a) 33-bus system



(b) 13-bus system



(c) 69-bus system

Fig. 4. DLMP calculated by DSOs

Fig. 4 shows that the DLMP received by each microgrid within the same DSO is different from each other. This is because each microgrid contains distributed generators (DG) with different generation costs, and the DLMP should be equal to the marginal cost of DG. The different compositions of microgrids may lead to various price signals. In addition, the DLMP and DG generations are time-varying. This is because the RES generation and demand of microgrids are fluctuating during real-time operation. In this simulation, the time resolution of wind speed, solar radiation and load is one minute. Hence the DLMP is adjusted accordingly to maintain the power exchange at PCC to a steady level.

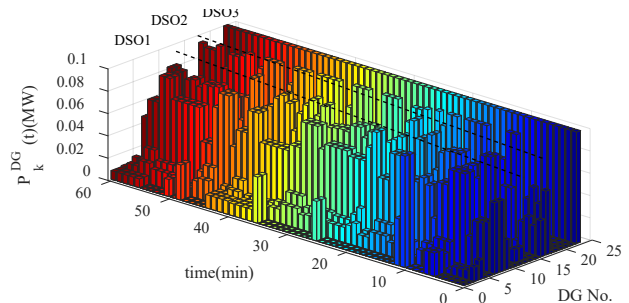


Fig. 5. DG generation under DLMP

C. Observations from the simulation study

The following observations can be made from our simulation:

1) **DLMP at marginal cost of DG:** The DLMP equals the marginal cost of the DG. For instance, at the 11–14 minutes, the DLMP for MG2 in the 69-bus system reaches a spike of 141.7\$/MWh. MG2 has two MTs numbered as 16 and 17 in Fig. 5. Their generation are 0.0535 MW and 0.1 MW, respectively. The marginal cost is $2 \times 1040 \times 0.0535 + 30.4 = 141.7$ \$/MWh and $2 \times 510 \times 0.1 + 39.7 = 141.7$ \$/MWh, which equal the DLMP.

2) **Constant DLMP:** The DLMP for some microgrids remains almost constant for the entire interval, e.g., MG1 in the 13-bus system and MG3 bus in the 33-bus system. This is because DGs in these microgrids have relatively high marginal cost, and the DSO intends to reach the cleared bid with the lowest possible expense. As a result, the expensive DGs are not dispatched and the DLMP equals the b coefficient in the cost function, as can be deduced from Eq. (27).

3) **High DLMP:** The DLMP for some MGs remains at a relatively high level, for example, MG5 in the 69-bus system. This is because the DGs in MG5 have a lower marginal cost, and it is dispatched for most of the time to reach the cleared bid, which is different from observation 2.

4) **Demand response participation:** In the above simulation, the demand response resources in microgrids have a relatively high dispatch cost compared with DGs and are barely dispatched by DSO. This is named as the base case. We further set the DR cost to 40\$/MWh, which is at the same level with DG cost, and DR participation result is shown in Fig. 6:

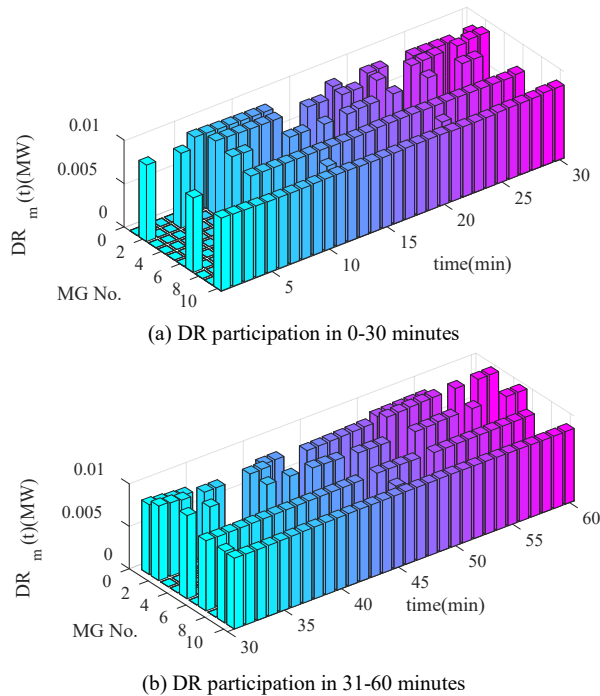


Fig. 6. DR participation in balancing market bidding

Fig. 6 demonstrates the DR performance in microgrids in all three DSOs. In the base case when little DR is dispatched, the total net power exchange between MGs and the DSO is 37.56 MW, from MGs to DSO. In the case when DR cost is decreased, the net power exchange increases to 40.15 MW. In this case, the cheaper DR is deployed for microgrids to make more profits by selling power back to the DSO.

5) **Power exchange following effect of microgrids:** Since the goal of the DSO is to stimulate local microgrids to constantly provide the exact amount of power exchange that equals the cleared bid, the power exchange following effects of local microgrids is examined. Results show that $\delta P_{PCC}^{RT}(t)$ remains around zero during the entire simulation hour for all three DSOs. This justifies that microgrids possess desirable response capability under proper price signals and are qualified to serve as power balancing resources for transmission systems.

6) **The performance of MLR:** At the transmission-level market bidding stage, the DSO applies an MLR method to decide the optimal bidding price. In our simulation, this is realized via MATLAB toolbox *regress*. Fig. 7 demonstrates the bidding quantity submitted by DSOs and the final market cleared quantity for all 12 sub-hourly time intervals, where there is no gap between the two. Therefore, the MLR approach is very effective in helping DSOs to decide the optimal bidding price and to win the desired market bid.

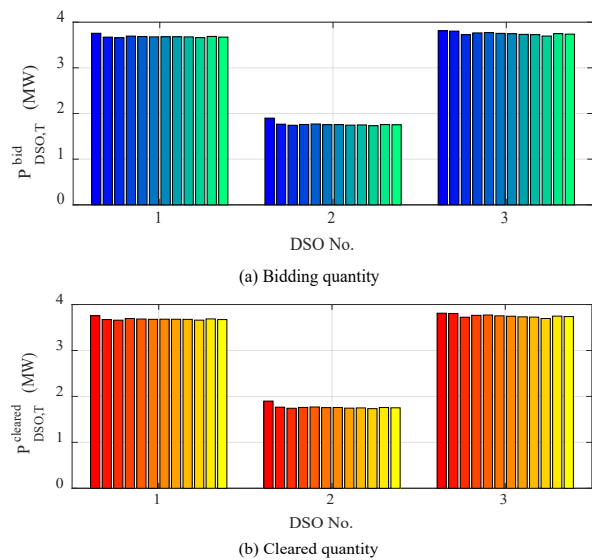


Fig. 7. Comparison of bidding quantity and market cleared quantity of DSO.

7) **Economic benefit of microgrids:** As stated in Section II-B, microgrid operators are independent and profit-driven entities. They can only form a contract with a DSO when there is extra benefit earned by participating in the balancing market. Hence, we compare the total operating cost for one hour of each microgrid between participating in balancing market with the DSO and when standing alone. The results are shown in TABLE III. As observed from the table, by responding to the DLMP, microgrids can reduce their operation cost; some microgrids even receive a large amount of extra profits by selling power to the DSO (shown as negative cost). Therefore, we can conclude that microgrids can operate with better economy by providing balancing service to the transmission system.

TABLE III COMPARISON OF MG OPERATION COST

System		Participating in Balancing market	Standing alone
DSO1 (33-bus system)	MG1	\$90.09	\$156.00
	MG2	\$21.28	\$161.21
	MG3	\$62.10	\$72.02
DSO2 (13-bus system)	MG1	\$35.33	\$48.00
	MG2	\$-100.87	\$51.55
DSO3 (69-bus system)	MG1	\$154.45	\$156.00
	MG2	\$-259.26	\$105.30
	MG3	\$46.39	\$49.42
	MG4	\$70.19	\$71.12
	MG5	\$-160.09	\$26.09

VI. CONCLUSION

In this paper, a hierarchical market framework is proposed to involve multiple microgrids with DSRs in real-time balancing market bidding. Microgrids can be driven by DLMPs sent from DSOs to provide the required amount of power in real-time operation via OPF calculation. At the distribution level of the proposed market framework, an MPCC model is established to combine the bi-level optimization of DSOs and microgrids into one problem for computational feasibility. At the transmission market bidding level, an MLR approach is applied to facilitate the DSO in optimal market bidding. The major conclusions from our simulation results are threefold:

1) Microgrids can follow the required power exchange profile with adequate accuracy and efficiency, which makes it a desirable balancing service provider to the transmission system in real-time scenario;

2) The proposed MLR method is highly effective in optimizing the bidding decision of DSO in balancing market to win the desired bid, so it can be an ancillary tool for DSOs and market bidders in real-world applications; and

3) It is highly profitable for DSR-driven microgrids to provide balancing services to the transmission systems, which quantitatively verifies that the proposed cause is beneficial to both local microgrids and transmission systems.

ACKNOWLEDGEMENT

This work was supported in part by the Engineering Research Center (ERC) Program of the U.S. National Science Foundation (NSF) and the Department of Energy (DOE) under NSF Award Number EEC-1041877 and the CURENT Industry Partnership Program.

REFERENCES

[1] Q. Shi, F. Li, Q. Hu, and Z. Wang, "Dynamic demand control for system frequency regulation: Concept review, algorithm comparison, and future vision," *Electric Power Systems Research*, vol. 154, pp. 75-87, 2018.

[2] S. Chua-Liang, and D. Kirschen, "Quantifying the Effect of Demand Response on Electricity Markets," *IEEE Trans. Power Syst.*, vol. 24, pp. 1199-1207, 2009.

[3] M. Parvania, M. Fotuhi-Firuzabad, and M. Shahidehpour, "Optimal Demand Response Aggregation in Wholesale Electricity Markets," *IEEE Trans. Smart Grid*, vol. 4, pp. 1957-1965, 2013.

[4] E. Mahboubi-Moghaddam, M. Nayeripour, J. Aghaei, A. Khodaei, and E. Waffenschmidt, "Interactive Robust Model for Energy Service Providers Integrating Demand Response Programs in Wholesale Markets," *IEEE Trans. Smart Grid*, vol. 9, pp. 2681-2690, 2018.

[5] J. Aghaei, and M.-I. Alizadeh, "Critical peak pricing with load control demand response program in unit commitment problem," *IET Generation, Transmission & Distribution*, vol. 7, pp. 681-690, 2013.

[6] J. Aghaei, and M.-I. Alizadeh, "Robust n-k contingency constrained unit commitment with ancillary service demand response program," *IET Generation, Transmission & Distribution*, vol. 8, pp. 1928-1936, 2014.

[7] X. Fang, Q. Hu, F. Li, B. Wang, and Y. Li, "Coupon-Based Demand Response Considering Wind Power Uncertainty: A Strategic Bidding Model for Load Serving Entities," *IEEE Trans. Power Syst.*, vol. 31, pp. 1025-1037, 2016.

[8] M. Gonzalez Vaya, and G. Andersson, "Self Scheduling of Plug-In Electric Vehicle Aggregator to Provide Balancing Services for Wind Power," *IEEE Trans. Sustain. Energy*, vol. 7, pp. 886-899, 2016.

[9] W. Pei, Y. Du, W. Deng, et al, "Optimal Bidding Strategy and Intramarket Mechanism of Microgrid Aggregator in Real-Time Balancing Market," *IEEE Trans. Ind. Informat.*, vol. 12, pp. 587-596, 2016.

[10] H. Farzin, R. Ghorani, M. Fotuhi-Firuzabad, and M. Moeini-Aghaie, "A Market Mechanism to Quantify Emergency Energy Transactions Value in a Multi-Microgrid System," *IEEE Trans. Sustain. Energy*, early access.

[11] H. S. V. S. K. Nunna, and D. Srinivasan, "Multiagent-Based Transactive Energy Framework for Distribution Systems With Smart Microgrids," *IEEE Trans. Ind. Informat.*, vol. 13, pp. 2241-2250, 2017.

[12] Y. Cai, T. Huang, E. Bompard, Y. Cao, and Y. Li, "Self-Sustainable Community of Electricity Prosumers in the Emerging Distribution System," *IEEE Trans. Smart Grid*, vol. 8, pp. 2207-2216, 2017.

[13] X. Hu, and T. Liu, "Co-optimisation for distribution networks with multi-microgrids based on a two-stage optimisation model with dynamic electricity pricing," *IET Generation, Transmission & Distribution*, vol. 11, pp. 2251-2259, 2017.

[14] L. Bai, J. Wang, C. Wang, C. Chen, and F. Li, "Distribution Locational Marginal Pricing (DLMP) for Congestion Management and Voltage Support," *IEEE Trans. Power Syst.*, vol. 33, pp. 4061-4073, 2018.

[15] Z. Wang, B. Chen, J. Wang, M. M. Begovic, and C. Chen, "Coordinated energy management of networked microgrids in distribution systems," *IEEE Trans. Smart Grid*, vol. 6, pp. 45-53, 2015.

[16] A. Saint-Pierre, and P. Mancarella, "Active Distribution System Management: A Dual-Horizon Scheduling Framework for DSO/TSO Interface Under Uncertainty," *IEEE Trans. Smart Grid*, vol. 8, pp. 2186-2197, 2017.

[17] S. Bahramara, M. Yazdani-Damavandi, J. Contreras, M. Shafie-Khah, and J. P. S. Catalao, "Modeling the Strategic Behavior of a Distribution Company in Wholesale Energy and Reserve Markets," *IEEE Trans. Smart Grid*, vol. 9, pp. 3857-3870, 2018.

[18] W.-Y. Chiu, H. Sun, and H. V. Poor, "A Multiobjective Approach to Multimicrogrid System Design," *IEEE Trans. Smart Grid*, vol. 6, pp. 2263-2272, 2015.

[19] I. Gorooi Sardou, M. E. Khodayar, K. Khaledian, M. Soleimani-damaneh, and M. T. Ameli, "Energy and Reserve Market Clearing With Microgrid Aggregators," *IEEE Trans. Smart Grid*, vol. 7, pp. 2703-2712, 2016.

[20] S. D. Manshadi, and M. E. Khodayar, "A Hierarchical Electricity Market Structure for the Smart Grid Paradigm," *IEEE Trans. Smart Grid*, vol. 7, pp. 1866-1875, 2016.

[21] H. Xu, K. Zhang, and J. Zhang, "Optimal Joint Bidding and Pricing of Profit-seeking Load Serving Entity," *IEEE Trans. Power Syst.*, early access, 2018.

[22] PJM Manual 11, Energy & Ancillary Services Market Operations, PJM, 2012 [Online]. Available: pjm.com/~media/documents/manuals/m11.ashx

[23] S. S. Guggilam, E. Dall'Anese, Y. C. Chen, S. V. Dhople, and G. B. Giannakis, "Scalable Optimization Methods for Distribution Networks with High PV Integration," *IEEE Trans. Smart Grid*, vol. 7, pp. 2061-2070, 2016.

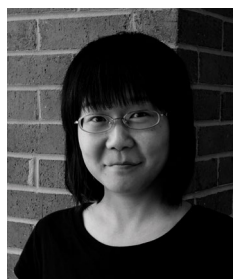
[24] G. Liu, Y. Xu, and K. Tomsovic, "Bidding Strategy for Microgrid in Day-Ahead Market Based on Hybrid Stochastic/Robust Optimization," *IEEE Trans. Smart Grid*, vol. 7, pp. 227-237, 2016.

[25] M. Parvania, and M. Fotuhi-Firuzabad, "Demand Response Scheduling by Stochastic SCUC," *IEEE Trans. Smart Grid*, vol. 1, pp. 89-98, 2010.

[26] Jager, D.; Andreas, A.; (1996). NREL National Wind Technology Center (NWTC): M2 Tower; Boulder, Colorado (Data); NREL Report No. DA-5500-56489. <http://dx.doi.org/10.5439/1052222>

[27] (Oct. 2016). Ercot Backcasted (Actual) Load Profiles-Historical. [Online]. Available: <http://www.ercot.com/mktinfo/loadprofile/alp>

[28] R. D. Zimmerman. (2010, February). Uniform Price Auctions and Optimal Power Flow. Mat-power Technical Note 1. [Online]. Available: <http://www.pserc.cornell.edu/matpower/TN1-OPF-Auctions.pdf>



Yan Du (S'16) received the B.S. degree from Tianjin University, Tianjin, China, and the M.S. degree from Institute of Electrical Engineering, Chinese Academy of Sciences, Beijing, China, in 2013, and 2016, respectively. She is currently working toward the Ph.D. degree at the University of Tennessee, Knoxville, TN, USA. Her research interests include distribution system operation and deep learning in power systems.



Fangxing Li (S'98-M'01-SM'05-F'17) is also known as Fran Li. He received the B.S.E.E. and M.S.E.E. degrees from Southeast University, Nanjing, China, in 1994 and 1997, respectively, and the Ph.D. degree from Virginia Tech, Blacksburg, VA, USA, in 2001.

Currently, he is the James McConnell Professor at the University of Tennessee, Knoxville, TN, USA. His research interests include renewable energy integration, demand response, power markets, power system control, and power system computing.